X-ray absorption near edge spectroscopy investigations of valency and lattice occupation site of Fe in highly iron-doped lithium niobate crystals

2006 J. Phys.: Condens. Matter 18 5135

(http://iopscience.iop.org/0953-8984/18/22/013)

INSTITUTE OF PHYSICS PUBLISHING JOURNAL OF PHYSICS: CONDENSED MATTER

J. Phys.: Condens. Matter **18** (2006) 5135–5146 doi:10.1088/0953-8984/18/22/013

X-ray absorption near edge spectroscopy investigations of valency and lattice occupation site of Fe in highly iron-doped lithium niobate crystals

Kh Olimov[1,2], M Falk[3], K Buse[3], Th Woike[3,4], J Hormes[1] and H Modrow[1]

[1] Institute of Physics, University of Bonn, Nussallee 12, 53115 Bonn, Germany
[2] Physical-Technical Institute of SPA 'Physics-Sun' of Uzbek Academy of Sciences, G Mavlyanova 2[b], 700084 Tashkent, Uzbekistan
[3] Institute of Physics, University of Bonn, Wegelerstrasse 8, 53115 Bonn, Germany
[4] Institute for Crystallography, University of Cologne, Zülpicherstrasse 49[b], D-50674 Cologne, Germany

E-mail: olimov@physik.uni-bonn.de

Received 2 March 2006, in final form 21 April 2006
Published 19 May 2006
Online at stacks.iop.org/JPhysCM/18/5135

Abstract

The oxidation state of Fe in highly doped lithium niobate crystals (2 wt% Fe_2O_3) in the as-grown, reduced, and oxidized states is determined by the combination of differentiation and integration methods applied to their Fe K-edge XANES (x-ray absorption near edge spectroscopy) spectra. The obtained valences are confirmed further by absorption measurements in the IR/vis (infrared and visible) spectral range. It is shown that reduction and thermo-electric oxidization of as-grown Fe:$LiNbO_3$, respectively, leads to a noticeable lowering of the number of Fe^{3+} and to complete oxidization of all Fe^{2+} to Fe^{3+}, respectively. It is found that Fe in highly iron-doped lithium niobate samples (0.5, 2, and 4 wt% Fe_2O_3) is incorporated onto the Li site comparing the experimental XANES spectra to the FEFF8 calculations. The difference of the XANES spectrum of the 4 wt% Fe_2O_3 doped sample as compared to those of the 0.5 and 2 wt% doped samples is explained by a co-phase formation in the former one. The results obtained can help to tailor such crystals for non-linear optical applications as well as for photorefraction.

1. Introduction

Lithium niobate crystals ($LiNbO_3$) are one of the most important electro-optical and nonlinear optical materials. Single crystals of $LiNbO_3$ are used, e.g., to fabricate efficient electro-optical and integrated-optical devices for telecommunication, such as phase and intensity modulators, directional couplers, and optical filters [1]. Furthermore, frequency doublers or mixers are realized with lithium niobate crystals, in particular using quasi-phase-matching [2]. However, several properties of this material depend strongly on the impurity centres in these crystals.

For example, transition metal ions, especially iron, were found to be responsible for the well known photorefractive effect, i.e. the light-induced refractive index changes [3]. The photorefractive effect can be useful to realize, e.g., volume holographic optical filters for telecommunication [4]. However, for nonlinear-optical applications strong suppression of the photorefractive effect is desired. Thus full control of the photorefractive properties is required.

Iron occurs in $LiNbO_3$ in the oxidation states Fe^{2+} and Fe^{3+} [5]. Illumination with visible light excites electrons from Fe^{2+} to the conduction band. The electrons are then redistributed because of the bulk photovoltaic effect, diffusion, and drift, and finally they are trapped elsewhere by Fe^{3+} [3]. However, this one-centre scheme was refined; namely, the intrinsic defects Nb_{Li} caused by non-stoichiometry of lithium niobate were shown to participate in the charge transport as shallow electron traps [6]. At low doping concentrations, the optical-damage-resistant impurities (Mg^{2+}, Zn^{2+}, In^{3+}, and Sc^{3+}) were shown to smoothly remove the electron traps Nb_{Li} and hence to reduce the space charge fields and the photorefractive effect [7].

Since the defects in doped $LiNbO_3$ and its photorefractive properties are highly correlated, the questions of interest are the site of incorporation of impurity ions into the lithium niobate lattice and their valences together with the favourable charge compensation mechanism [8, 9]. It is known that most impurity ions prefer incorporation at one specific site, most probably either a Li or Nb site. Impurity incorporation at interstitial sites, according to calculations, is energetically costly and, in addition, is unstable as impurity interstitials displace neighbouring Li ions along the *c* axis into nearby interstitial sites with the impurity being finally located at a Li site [8]. As is known for low doping concentrations, in congruent $LiNbO_3$ both Fe^{2+} and Fe^{3+} ions incorporate onto the Li site [10–12]. For high doping concentrations of iron and for different preparation treatments such as reduction and oxidization of the as-grown Fe:$LiNbO_3$, which are the subject of this investigation, the incorporation site for Fe for concentrations as high as 4 wt% Fe_2O_3 in lithium niobate crystals and also its valency have not been determined so far. Highly iron-doped lithium niobate crystals can be of interest for nonlinear-optical applications, where a thermo-electric oxidization treatment can reduce the Fe^{2+} concentration to get good transparency for visible light [13], while still maintaining enough electrons to provide, through tunnelling of electrons between iron centres [14], a large dark conductivity that suppresses the photorefractive effect. Furthermore, highly doped as-grown and reduced crystals show a new kind of charge transport, so-called 'polar currents', caused by the polarity of the material and recombination of electrons within an impurity band [15].

In the present work x-ray absorption near edge spectroscopy (XANES) is used to determine the site of incorporation of Fe and also its oxidation state in lithium niobate crystals highly doped with Fe in the as-grown state and after various treatments. XANES probes the local chemical and thus the electronic environment of the excited atom. No long range order in the samples is required, unlike in XRD (x-ray diffraction) analysis, and amorphous as well as crystalline samples can be investigated using XANES [16, 17]. Especially at the K edge of an absorbing atom, some strong resonances appear below the ionization potential, and they are assigned to electron transitions from the 1s orbital to unoccupied electron states below the ionization potential [16–18]. Since the energy position of the absorption edge and of the ionization threshold transition (1s to continuum) are very sensitive to the valency of the absorbing atom, this technique can be used to determine the oxidation state of the absorbing atom [18].

2. Experimental details

Single crystals of congruently melting $LiNbO_3$ doped with nominally 0.5, 2, and 4 wt% iron oxide (Fe_2O_3), which are denoted hereinafter as 0.5, 2, and 4 wt% Fe:$LiNbO_3$, were used. The

crystals were cut into samples of $7 \times 9 \times 1$ mm^3 size. In addition, reduction and oxidization of 2 wt% Fe:$LiNbO_3$ samples were performed. The reduction was done in a pure hydrogen atmosphere of a pressure of 10^{-3} mbar, where the crystal was heated up to 980 °C and kept for 24 h. The purity of the atmosphere was analysed with a mass spectrometer, and the partial pressure of all other elements was below 10^{-9} mbar. To oxidize the crystal, a thermo-electric oxidization method was used [13]. The crystal was heated with a heating ramp of 3 °C min^{-1} up to 700 °C and kept for 6 h. Afterwards, the crystal was cooled down to room temperature with a cooling ramp of -3 °C min^{-1}. The procedure was performed in air. During the whole annealing process a voltage of 1000 V was applied and the current was limited to 0.1 mA. At elevated temperatures the conductivities become so high that the voltage was reduced to avoid currents higher than 0.1 mA. During cooling the voltage was rising with decreasing conductivity.

The XANES spectra of the samples were obtained at the INE beamline at ANKA, operating in storage mode at 2.5 GeV with an average current of about 200 mA. The reference samples used were prepared from iron oxide powders FeO, Fe_3O_4, and Fe_2O_3 purchased from Sigma-Aldrich and having the purities 99, 98, and 99%, respectively. The x-ray beam was monochromatized using a double-crystal x-ray monochromator of the Lemmonier type [19] equipped with a pair of Ge(220) crystals having a $2d$ of 4 Å. The possible impact of higher orders was checked by detuning the crystals, and no influence was found. The spectra were recorded in fluorescence mode with an ionization chamber acting as a monitor of the incoming beam. The fluorescence radiation from the sample was detected by a five-element Ge detector. Absorption was recorded as the ratio of the fluorescence signal current of a Ge detector and the current of the monitor chamber as a function of the incoming photon energy. More details on this experimental set-up can be found in [20]. The XANES spectra were recorded with the incidence angle of the incoming x-ray beam onto the sample surface equal to 45°. To check the influence of polarization/orientation effects, the test XANES measurements of the samples for incidence angles equal to 15° and 60° were made and no influence of polarization/orientation effects on the measured XANES spectra was found. During the measurements, the photon energy was varied from 7050 to 7300 eV with energy steps of 0.4 eV and an integration time of about 2 s per step. The experimental spectra were calibrated relative to the energy of the Fe K edge, $E = 7112$ eV, determined as the first inflection point of the XANES spectrum of a Fe foil. Each sample was studied at least three times, and the reproducibility of the obtained spectra was confirmed. Then the corresponding spectra were added and averaged for better statistics. Since the background rise due to the fluorescence in the post-edge region was negligible for all XANES spectra, a linear fit was carried out in the region of 7060–7090 eV of the spectra and subtracted from the raw data. The spectra were then normalized to 1 at $E = 7177$ eV.

The absorption edge positions of the samples were determined in two ways. In a first method, an edge position was determined as the position of the first maximum in the differentiated spectrum. In a second approach, the absorption edge positions were determined in a procedure similar to that described by Capehart *et al* [21] and Sham *et al* [22]. The absorption spectrum was integrated up to the energy at which the value of absorption of the normalized spectrum reaches 1 for the first time. Hereinafter, the value of this integral is called the total integrated absorption. The energy position at which this integral attains 90% of the total integrated absorption was fixed as the respective edge position. Being relatively simple to implement, both methods have their disadvantages. In the first approach, a pre-edge feature may be perturbed by a $1s \rightarrow nd$ transition such that the threshold region is not representative for the dominant $1s \rightarrow np$ component of the edge structure [21]. The second method is certainly less arbitrary when dealing with various spectra, each possessing different near-edge structures,

but care should be taken to eliminate the white line contribution in most of the total integrated absorption spectra [18]. This is achieved by using approximately 80% or higher percentage of the total integrated absorption, before the normalized spectrum reaches unity for the first time, for fixing the respective edge position [21]. As long as the absorption in this region is dominated by transitions to (s, p)-like states, this method should be applicable [21]. The advantage of using both methods in the present work was that it allowed us to make consistency checks of the oxidation state of Fe of the samples obtained using the two different approaches. The consistency obtained allowed us, in its turn, to calculate from both methods the average oxidation state of Fe.

Measurements of the absorption coefficient of reduced, as-grown, and oxidized 2 wt% Fe:$LiNbO_3$ samples were performed in a transmission mode using a Cary 500 spectrometer in the IR/vis spectral range. For the absorption measurements of the crystals in the as-grown state a thin plate with a thickness of 55 μm was used. The absorption coefficient measurements for the as-grown and oxidized samples were made at 477 nm. Since the absorption at 477 nm was too high for the reduced crystal to detect any transmitted intensity, its absorption coefficient was measured at 1127 nm instead. Then the absorption coefficient was calculated for 477 nm using the linear correlation between the absorption at 477 and 1127 nm expressed by the formula $\alpha_{477\ \mathrm{nm}} = 1.9\ \mathrm{mm}^{-1} + 14.8\alpha_{1127\mathrm{nm}}$, where $\alpha_{477\ \mathrm{nm}}$ and $\alpha_{1127\ \mathrm{nm}}$ are the absorption coefficients in units of mm^{-1} at 477 and 1127 nm, respectively. To derive this formula, the values for absorption at 477 and 1127 nm from the widely accepted paper of Kurz *et al* [5] were plotted, and the linear regression was taken. Using the known relation [5] between Fe^{2+} concentration and the absorption at 477 nm, $c_{Fe^{2+}} = 2.16 \times 10^{21}\ \mathrm{m}^{-2}\alpha_{477\ \mathrm{nm}}$, the concentration of Fe^{2+} was calculated for the reduced, as-grown, and oxidized samples. An independent measurement by atomic absorption spectroscopy of the 2 wt% Fe:$LiNbO_3$ sample leads to a total iron concentration of 1.11 ± 0.03 wt%. The oxidation state of Fe for the samples was obtained from the calculated ratio $c_{Fe^{2+}}/c_{Fe}$, where c_{Fe} is the total iron concentration in the sample.

To interpret the experimental XANES spectra, XANES and LDOS (L-projected density of states) calculations were conducted using a real-space full multiple scattering approach using the FEFF8 code [23]. The results of this type of calculations for a cluster of typically 100 atoms proved to be reliable and allowed semiquantitative reproduction of almost all features of the transition-metal-compound XANES spectra at the metal K edges [18, 24]. For the purpose of this work, the XANES and PDOS (P density of states) calculations were done for a cluster of 100 atoms around Fe on Li and Nb sites in the $LiNbO_3$ matrix constructed according to $LiNbO_3$ structure data. The trigonal R_{3c} crystal structure with the cell parameters $a = b = 5.14$ Å and $c = 13.86$ Å [25] was used for constructing the $LiNbO_3$ matrix. The calculations were performed for a perfect crystal at $T = 0$ K and no experimental broadening was applied, because an improved agreement between experiment and theory is compensated for by loss of information obtainable from the calculated spectrum [18]. To perform FEFF8 calculations, the default settings were used for the EXCHANGE card, which implies the use of Hedin–Lundqvist self-energy as the exchange–correlation potential. Apart from this, the only cards used were SCF (self-consistent potential), FMS (full multiple scattering) and XANES as well as LDOS, which was calculated in the range between -30 and 30 eV with a resolution of 0.1 eV. The muffin-tin radii used for calculations were 1.367, 0.990, 1.289, and 1.279 Å for atoms of Fe, O, Nb, and Li, respectively. The radius of the cluster used in the SCF procedure was 4.0 Å, which corresponds to the cluster of about 30 at. around the central absorbing Fe atom in the $LiNbO_3$ matrix.

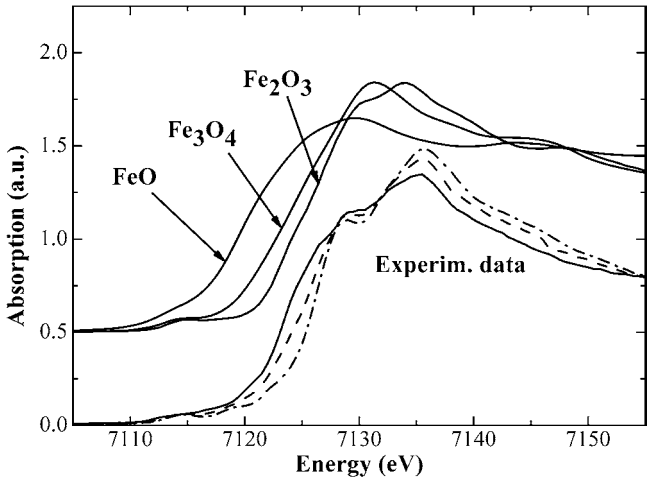

Figure 1. Experimental XANES spectra of a 2 wt% Fe:$LiNbO_3$ crystal (reduced (solid line), as grown (dashed line), and oxidized (dashed–dotted line)) along with the reference spectra.

Table 1. The XANES results of the Fe oxidation state.

2 wt% Fe:$LiNbO_3$	Differentiation	Integration	Average oxidation state of Fe
Reduced	2.6 ± 0.1	2.8 ± 0.2	2.7 ± 0.1
As-grown	2.8 ± 0.1	2.9 ± 0.2	2.9 ± 0.1
Oxidized	2.9 ± 0.1	3.1 ± 0.3	3.0 ± 0.2

3. Determination of Fe valences in the as-grown, reduced, and oxidized states of Fe:$LiNbO_3$

In figure 1 the experimental XANES spectra of reduced, as-grown, and oxidized 2 wt% Fe:$LiNbO_3$ are presented along with those of Fe oxide references. The dependence of the absorption edge of Fe on its formal valence can be clearly seen in figure 1: the absorption edge of Fe oxide shifts to higher energy with an increase of Fe valence. This is in agreement with an empirical law mentioned already in [26–28]. The absorption edge positions of reduced, as-grown, and oxidized 2% Fe:$LiNbO_3$ samples are well separated from each other and shift to higher energies as one goes from reduced to as-grown, and further to oxidized 2% Fe:$LiNbO_3$. Comparing the absorption edge positions of these crystals with those of the reference iron oxides, one can see that the reduced sample has an oxidation state close to that of Fe_3O_4, whereas as-grown and oxidized samples have an oxidation state close to the trivalent Fe_2O_3, the oxidized one having the absorption edge at slightly higher energy than the as-grown one.

To quantify these qualitative findings on the oxidation state of Fe in $LiNbO_3$, we evaluated the Fe valence for these samples using Fe oxides with known oxidation state of Fe as references applying the differentiation and integration method described above. The oxidation state of Fe for reduced, as-grown, and oxidized 2% Fe:$LiNbO_3$ was determined based on a scale obtained from a linear fit of the absorption edge position of the reference oxides with known valences. One can see the results in table 1 and figure 2.

The results in table 1 confirm the qualitative trend observed from the relative positions of the absorption edges of the samples in figure 1. The relatively large errors of the obtained Fe valences are caused mainly by uncertainties at the determination of the slope parameter of the

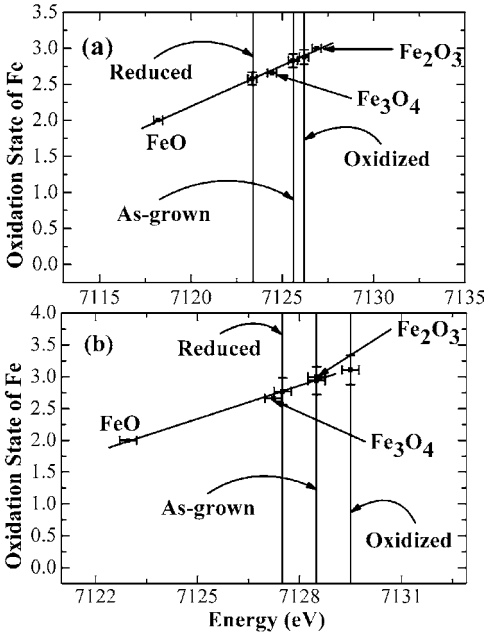

Figure 2. Determination of the Fe oxidation state for reduced, as-grown, and oxidized 2 wt% Fe:$LiNbO_3$ based on differentiation (a) and integration (b) methods (the horizontal error bars are the experimental errors of energy determination). $Y = A + BX$ linear fit parameters are $A = -805.14 \pm 51.46$ (a.u.), $B = 0.113 \pm 0.007$ (a.u. eV^{-1}), for differentiation, and $A = -1236.91 \pm 149.86$ (a.u.), $B = 0.17 \pm 0.02$ (a.u. eV^{-1}), for the integration method.

Table 2. The IR/vis absorption spectroscopy results of the Fe oxidation state.

2 wt% Fe:$LiNbO_3$	Absorption at 477 nm (mm^{-1})	$c_{Fe^{2+}}$ (10^{26} m^{-3})	$c_{Fe^{2+}}/c_{Fe}$	Oxidation state of Fe
Reduced	60.6 ± 0.2	1.3 ± 0.4	0.3 ± 0.1	2.7 ± 0.4
As-grown	47.7 ± 0.2	1.0 ± 0.3	0.2 ± 0.1	2.8 ± 0.3
Oxidized	0.7 ± 0.1	0.015 ± 0.005	$<0.004 \pm 0.001$	$3.0 \pm 0.0(1)$

linear fit. Note that these are intrinsic to the method, as e.g. edge positions of spectra with identical formal valency can vary slightly as a function of lattice structure [18]. As one can see in figure 2, the positions of the absorption edge of the samples given by vertical lines are separated well considering the values of the experimental energy errors given by horizontal bars, as was also seen in their experimental XANES spectra in figure 1. Thus, the changes in valency are significant, whereas the obtained absolute values are influenced by the method of choice.

The above obtained results on the Fe oxidation state are compared with those from IR/vis absorption spectroscopy. The IR/vis absorption spectroscopy results for reduced, as-grown, and oxidized 2 wt% Fe:$LiNbO_3$ are presented in table 2. The IR/vis absorption measurements revealed the presence of both Fe^{2+} and Fe^{3+}, in the reduced and as-grown states of the crystal, whereas in the case of the oxidized crystal almost no Fe^{2+} was left. The Fe valency obtained from the IR/vis absorption measurements for the reduced crystal agrees well with the corresponding average oxidation state in table 1 obtained from the XANES measurements. The Fe valency for the as-grown crystal obtained from IR/vis absorption measurements differs

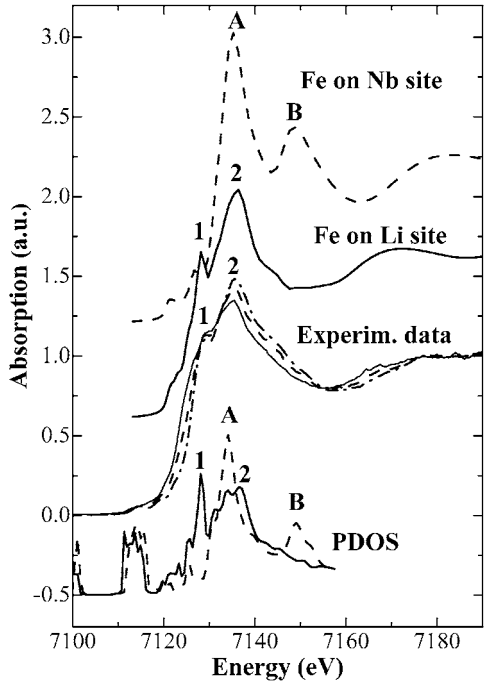

Figure 3. Experimental XANES spectra of 2 wt% Fe:$LiNbO_3$ (reduced (solid line), as grown (dashed line), and oxidized (dashed–dotted line)) along with XANES and PDOS calculations using FEFF8 code. The calculated position of the Fermi energy is 7120.9 and 7120.4 eV for Fe-on-Li-site and Fe-on-Nb-site PDOS calculations, respectively.

from that in table 1, but still agrees to within the error ranges. The oxidation state of Fe in the oxidized crystal obtained from IR/vis absorption measurements, $3.0 \pm 0.0(1)$, agrees perfectly with the corresponding value obtained from XANES, 3.0 ± 0.2, which confirms that all Fe^{2+} is oxidized to Fe^{3+} during the thermo-electric oxidization method applied to the as-grown Fe:$LiNbO_3$ [13].

4. Determination of the site of Fe incorporation

In figure 3 one can see the experimental XANES spectra of reduced, as-grown, and oxidized 2% Fe:$LiNbO_3$ samples along with XANES calculations using the FEFF8 code. Feature 1 and maximum 2 of the experimental spectra can be related to structure 1 and maximum 2 of the Fe-on-Li-site calculations. These structures are sharper in the calculated spectrum than in the experiment because of not taking into account the experimental broadening effect in the calculations. As is evident from figure 3, Fe-on-Nb-site XANES calculations differ significantly from the experimental spectra. There is no structure of sufficient intensity in these calculations to reproduce feature 1 in the experimental spectra. Also, no indication is found if one looks for the strong structure B in the experimental spectra. Thus comparison of the experimental spectra to calculations favours strongly Li site occupation by Fe in 2 wt% Fe:$LiNbO_3$. This is in agreement with the results mentioned already in [10–12]. Since in the experiment the dipole allowed $1s \rightarrow np$ excitations of 1s electrons are probed, the PDOS (P density of states) calculations for Fe on Li and on Nb sites are also shown in figure 3. With

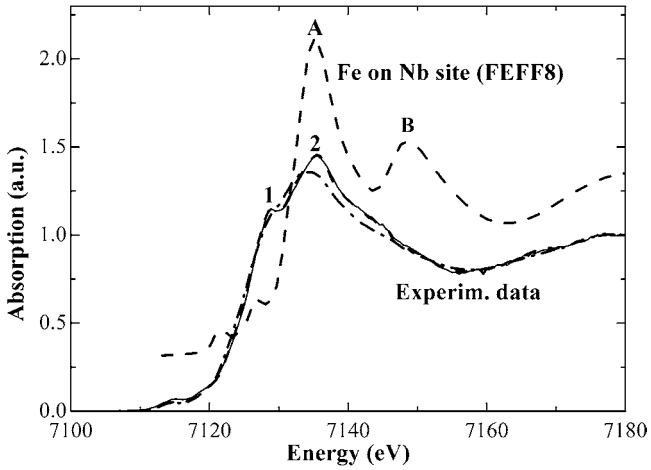

Figure 4. Experimental XANES spectra of as-grown Fe:$LiNbO_3$ at different iron concentrations (0.5 wt% (solid thin line), 2 wt% (dashed line), and 4 wt% of Fe_2O_3 (dashed–dotted line)) along with FEFF8 calculations.

regard to the structures below approximately 7115 eV, they lie below the Fermi energy and show the density of already occupied states where the 1s electron cannot be excited during an x-ray absorption process. Hence these structures do not show up in the measured XANES spectra.

Now we turn to the XANES spectra of as-grown Fe:$LiNbO_3$ at different iron concentrations, which are depicted in figure 4. As can be seen from this figure, the experimental XANES spectra of 0.5 and 2 wt% Fe:$LiNbO_3$ coincide. This suggests that 0.5 and 2 wt% Fe:$LiNbO_3$ have a similar structure. Hence one can conclude that Fe atoms also occupy the Li site in the $LiNbO_3$ in the case of the 0.5 wt% Fe:$LiNbO_3$ sample.

5. Co-phase formation for very high iron concentrations

For the 4 wt% Fe:$LiNbO_3$ sample, the XANES spectrum differs noticeably from that of the 0.5 and 2 wt% Fe:$LiNbO_3$ crystals. For example, feature 1 of the 4 wt% sample is less pronounced, and the position of the maximum of structure 2 is shifted to lower energies and its intensity is lowered.

There are two possible reasons for the change of the structure of the 4 wt% Fe:$LiNbO_3$ crystal, as compared to those of the 0.5 and 2 wt% Fe:$LiNbO_3$ crystals: (a) Nb site occupation by Fe; (b) co-phase formation. Comparing the experimental XANES spectrum of 4 wt% Fe:$LiNbO_3$ with Fe-on-Nb-site XANES calculations shown in figure 4, one does not see any indication of a highly pronounced structure B in the experimental spectrum. Thus Nb site occupation by Fe in the case of the 4 wt% sample, i.e. variant (a), is very unlikely. Let us then check also whether the changes observed in the XANES spectrum of the as-grown 4 wt% Fe:$LiNbO_3$ sample could be explained simply by non-homogeneous distribution of iron ions on the Li site in the $LiNbO_3$ matrix. To check this possibility, several Fe-on-Li-site XANES calculations were done for a cluster of 100 at. in $LiNbO_3$ matrix with only one central absorbing Fe atom, with 50% of Li atoms replaced by Fe atoms, and with 100% of Li atoms replaced by Fe atoms (which would be an extreme unrealistic case with much higher Fe concentrations than in the sample). As observed in figure 5, these calculations cannot describe the changes

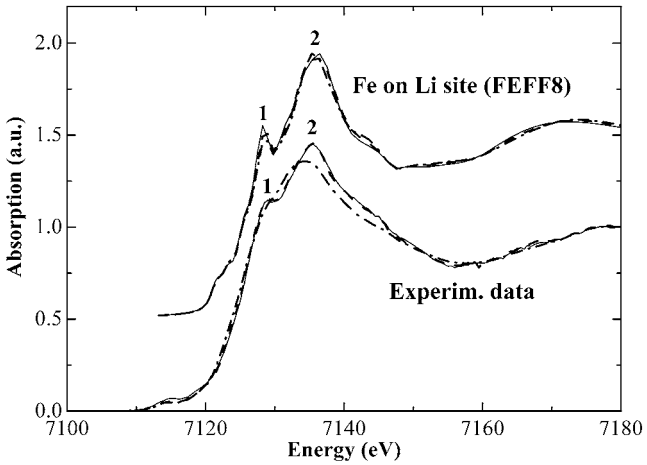

Figure 5. The Fe-on-Li-site XANES calculations using the FEFF8 code for only one central absorbing Fe atom (solid thin line), for 50% of Li atoms replaced by Fe atoms (dashed line), and for 100% of Li atoms replaced by Fe atoms (dashed–dotted line) in the $LiNbO_3$ matrix along with the experimental XANES spectra of as-grown Fe:$LiNbO_3$ at different iron concentrations (the same as in figure 4).

observed in the XANES spectrum of the as-grown 4 wt% Fe:$LiNbO_3$ sample as compared to those of 0.5 and 2 wt% Fe:$LiNbO_3$ samples. Thus the non-homogeneous distribution of iron ions on the Li site in the $LiNbO_3$ matrix can hardly be responsible for these changes.

For variant (b), or co-phase formation, we propose a model according to which upon an increase of the Fe content up to the threshold value corresponding to the number of vacant Li sites Fe occupies only the Li site in $LiNbO_3$. This can explain, for example, the identity of the experimental XANES spectra of 0.5 and 2 wt% Fe:$LiNbO_3$. Then, according to the model, upon further increase of the Fe content above the threshold value, i.e. after all Li vacancies are filled by Fe, Fe atoms start forming the co-phase. To maintain the charge neutrality in the highly iron-doped lithium niobate crystals, the charge compensation may proceed by a co-phase formation of Fe_2O_3. The experimental XANES spectra of α-Fe_2O_3 and γ-Fe_2O_3 along with that of 4 wt% Fe:$LiNbO_3$ are shown in figure 6. The closeness of the edge position and behaviour of XANES spectra of both α-Fe_2O_3 and γ-Fe_2O_3 to that of 4 wt% Fe:$LiNbO_3$ further supports the idea of using Fe_2O_3 as the model co-phase.

Let us quantify the model assumptions. There are about 0.8 at.% Li vacancies in congruent non-stoichiometric $Li_{0.95}Nb_{1.01}O_3$ [29–31] and approximately 2 at.% of Fe in 4 wt% Fe:$LiNbO_3$ sample. If 0.8 at.% Fe atoms fill all the Li vacancies, then the remaining 1.2 at.% Fe atoms can be used to form the co-phase. Thus, according to the estimations, the XANES spectrum of 4 wt% Fe:$LiNbO_3$ could be represented as a mixture of the XANES spectra of 40% of Fe:$LiNbO_3$ with pure Li site occupation by 0.8 at.% Fe, and 60% of co-phase compound formed by the other 1.2 at.% Fe.

As shown in figure 7, the mixture of 60% of Fe_2O_3 and 40% of 0.5 wt% Fe:$LiNbO_3$ spectra describes the experimental spectrum of 4 wt% Fe:$LiNbO_3$ quite well, which supports our model assumptions. The fit using gamma Fe_2O_3 seems to reproduce slightly better the absorption edge of 4 wt% Fe:$LiNbO_3$ as compared to that with alpha Fe_2O_3. The experimental spectrum is fitted well in the whole XANES region except at the energy region around 7146 eV, where the fits overestimate the experiment. This fit overestimation is bigger in the case of a γ-Fe_2O_3 co-phase than an α-Fe_2O_3 co-phase.

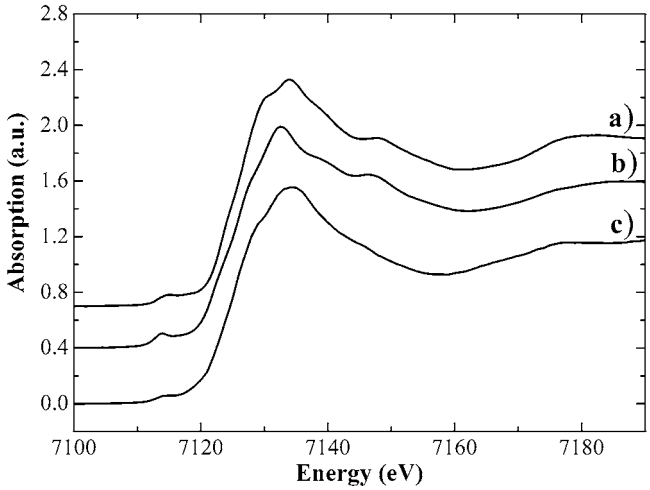

Figure 6. The experimental XANES spectra of α-Fe_2O_3 (a), γ-Fe_2O_3 (b), and as-grown 4 wt% Fe:$LiNbO_3$ (c).

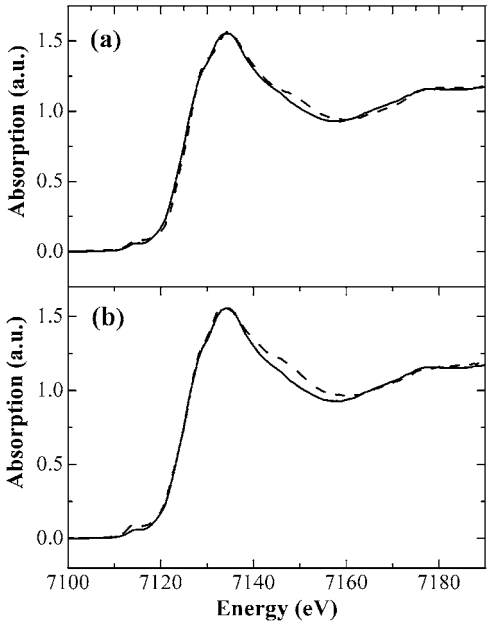

Figure 7. Fit (dashed line) of the 4 wt% Fe:$LiNbO_3$ (as-grown crystal) absorption spectrum (solid line) by a mixture of 60% α-Fe_2O_3 (a) or γ-Fe_2O_3 (b) and 40% of 0.5 wt% Fe:$LiNbO_3$ (as-grown crystal) absorption spectra. Note that experimental XANES spectra of alpha and gamma Fe_2O_3 samples of macroscopic cluster size were used for this fit procedure.

One of the reasons for this discrepancy can be the size of the oxide cluster formed since the XANES spectra are known to be sensitive to the cluster size. To check how the size of the Fe_2O_3 cluster can influence its XANES spectra, the shell-by-shell XANES calculations for both α-Fe_2O_3 and γ-Fe_2O_3 were performed. The calculations for α-Fe_2O_3 and γ-Fe_2O_3 are shown in figure 8. As observed in figure 8, the structure marked by arrows at the energies around 7145 eV

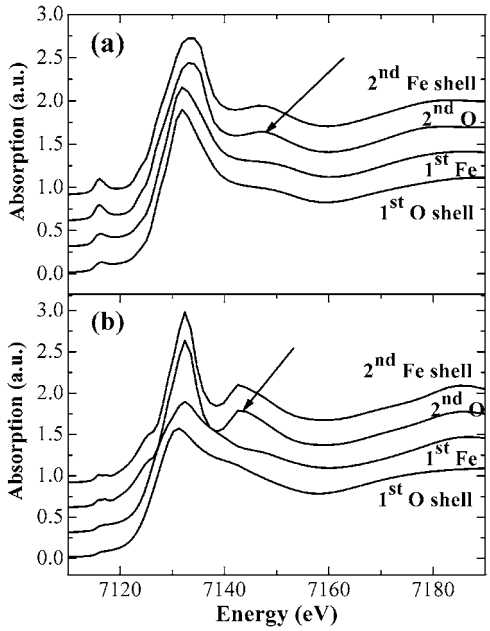

Figure 8. Shell-by-shell XANES calculations using FEFF8 code for α-Fe_2O_3 (a) and γ-Fe_2O_3 (b).

starts forming just after constructing the second oxygen shell around the absorbing Fe for both types of oxides. Hence the fit overestimation observed in the same region in figure 7 may be explained by the small cluster size of the oxide phase formed since the experimental XANES spectra of macroscopic size alpha and gamma iron oxides were used for this fit procedure. As evident from figure 8, the intensity of the structure marked by arrows is noticeably higher for gamma Fe_2O_3 than for alpha Fe_2O_3. This can explain the larger fit overestimation observed in the case of gamma Fe_2O_3 as compared to that of the alpha Fe_2O_3 model co-phase in figure 7.

6. Summary

The XANES spectra of highly iron-doped $LiNbO_3$ crystals were analysed. The oxidation state of Fe was determined for reduced, as-grown, and oxidized 2 wt% Fe:$LiNbO_3$ crystals based on both differentiation and integration methods and using the XANES spectra of the Fe oxides as the references. The oxidation state of Fe was found to be 2.7 ± 0.1, 2.9 ± 0.2, and 3.0 ± 0.2 for reduced, as-grown, and oxidized 2 wt% Fe:$LiNbO_3$ samples, respectively. The valences of Fe obtained from IR/vis absorption measurements for reduced (2.7 ± 0.4) and oxidized ($3.0 \pm 0.0(1)$) samples agree perfectly with the corresponding oxidation states obtained from XANES. This shows especially that a noticeable diminishing of the number of Fe^{3+} and complete oxidization of all Fe^{2+} to Fe^{3+} is achieved during the reduction and thermo-electric oxidization treatment, respectively, applied to the as-grown highly iron-doped lithium niobate crystals. XANES spectra were calculated for a cluster of 100 at. for Fe-on-Li and Fe-on-Nb sites in the $LiNbO_3$ matrix using the FEFF8 code. Comparing the experimental XANES spectra with the calculations, we found that Fe occupies the Li site in $LiNbO_3$ for 0.5 and 2.0 wt% Fe:$LiNbO_3$ samples, whereas the absorption spectrum and structure of 4 wt% Fe:$LiNbO_3$ differ noticeably from them. To describe the structure of 4 wt% Fe:$LiNbO_3$, a

model was proposed according to which upon an increase of Fe content higher than a threshold value, corresponding to the number of the vacant Li sites in lithium niobate, Fe atoms start forming a co-phase. Trivalent iron oxide (both α-Fe_2O_3 and γ-Fe_2O_3) was used as the model co-phase. The XANES spectrum of 4 wt% Fe:$LiNbO_3$ can be described well by a mixture of 60% of Fe_2O_3 and 40% of 0.5 wt% Fe:$LiNbO_3$ (with a pure Li site occupation by Fe) spectra, which agrees perfectly to the model estimations based on the number of the Li vacancies in congruent lithium niobate. The remaining discrepancies between the model fit and the experimental spectrum can be explained by the small size of the co-phase formed.

Acknowledgment

The authors gratefully acknowledge financial support by DFG for projects B1 and C4 within the DFG research unit 557 'Light confinement and control with structured dielectrics and metals'.

References

[1] Alferness R C, Burns W K, Donnelly J P, Kaminow I P, Kogelnik H, Leonberger F J, Milton A F, Tamir T and Tucker R S 1988 and 1990 *Guided-Wave Optoelectronics* ed T Tamir (Berlin: Springer)
[2] Fejer M M, Magel G A, Jundt D H and Byer R L 1992 *IEEE J. Quantum Electron.* **28** 2631
[3] Günter P and Huignard J 2005 *Photorefractive Materials and Their Applications* vol 1, ed J Huignard (Berlin: Springer)
[4] Boffi P, Piccinin D and Ubaldi M C 2002 *Infrared Holography for Optical Communications: Techniques, Materials and Devices* ed P Boffi (Berlin: Springer)
[5] Kurz H, Krätzig E, Keune W, Engelmann H, Gonser U, Dischler B and Rauber A 1977 *Appl. Phys.* **12** 355
[6] Jermann F and Otten J 1993 *J. Opt. Soc. Am.* B **10** 2085
[7] Bryan D A, Gerson R and Tomaschke H E 1984 *Appl. Phys. Lett.* **44** 847
[8] Donnerberg H, Tomlinson S M, Catlow C R A and Schirmer O F 1991 *Phys. Rev.* B **44** 4877
[9] Volk T, Maximov B, Sulyanov S, Rubinina N and Woehlecke M 2003 *Opt. Mater.* **23** 229
[10] Rebouta L, Dasilva M F, Soares J C, Hageali M, Stoquert J P, Siffert P, Sanzgarcia J A, Dieguez E and Agullolopez F 1991 *Europhys. Lett.* **14** 557
[11] Bush T S, Catlow C R A, Chadwick A V, Cole M, Geatches R M, Greaves G N and Tomlinson S M 1992 *J. Mater. Chem.* **2** 309
[12] Kling A, Soares J C and DaSilva M F 1995 *Insulating Materials for Optoelectronics New Developments* ed F Agullo-Lopez (New York: World Scientific)
[13] Falk M and Buse K 2005 *Appl. Phys.* B **83** 853
[14] Nee I, Müller M, Buse K and Krätzig E 2000 *J. Appl. Phys.* **88** 4282
[15] Beyer O, von Korff Schmising, Luenemann M, Buse K and Sturman B 2006 *Opt. Express* **14** 1533
[16] Bianconi A, Inoccia L and Stipcich S 1983 *EXAFS and Near Edge Structure* (*Springer Series in Chemical Physics* vol 27) (Berlin: Springer)
[17] Koningsberger D C and Prins R 1988 *X-ray Absorption: Techniques of EXAFS SEXAFS and XANES* (New York: Wiley)
[18] Pantelouris A, Modrow H, Pantelouris M, Hormes J and Reinen D 2004 *Chem. Phys.* **13** 300
[19] Lemmonier M, Collet O, Depautex C, Esteva J M and Raoux D 1978 *Nucl. Instrum. Methods* **152** 108
[20] Denecke M A, Rothe J and Dardenne K 2005 *Phys. Scr.* T **115** 1001
[21] Capehart T W, Herbst J F, Mishra R K and Pinkerton F E 1995 *Phys. Rev.* B **52** 7907
[22] Sham T K 1987 *Solid State Commun.* **64** 1103
[23] Ankudinov A, Ravel B, Rehr J J and Conradson S 1998 *Phys. Rev.* B **58** 7565
[24] Modrow H, Bucher S, Rehr J J and Ankudinov A L 2003 *Phys. Rev.* B **67** 035123
[25] Postnikov A V, Caciuc V and Borstel G 2000 *J. Phys. Chem. Solids* **61** 295
[26] Pantelouris A, Kueper G, Hormes J, Feldmann C and Jansen M 1995 *J. Am. Chem. Soc.* **117** 11749
[27] Wong J, Lytle F W, Messmer R P and Maylotte D H 1984 *Phys. Rev.* B **30** 5595
[28] Mande C and Sapre V B 1983 *Advances in X-ray Spectroscopy* vol 17 (New York: Pergamon)
[29] Abrahams S and Marsh P 1986 *Acta Crystallogr.* B **42** 61
[30] Iyi N, Kitamura K, Izumi F, Yamamoto J K, Hayashi T, Asano H and Kimura S 1992 *J. Solid State Chem.* **101** 340
[31] Zotov N, Boysen H, Schneider J and Frey F 1994 *Mater. Sci. Forum* **166–169** 631